Fullerenes as Tilings of Surfaces

M. Deza,*,† P. W. Fowler,*,‡ A. Rassat,*,§ and K. M. Rogers*,‡

Laboratoire d'Informatique, Ecole Normale Supérieure, 45 Rue d'Ulm, 75230 Paris, France, School of Chemistry, University of Exeter, Stocker Road, Exeter EX4 4QD, U.K., and Department of Chemistry, Ecole Normale Supérieure, Rue Lhomond, 75005 Paris, France

Received July 2, 1999

If a fullerene is defined as a finite trivalent graph made up solely of pentagons and hexagons, embedding in only four surfaces is possible: the sphere, torus, Klein bottle, and projective (elliptic) plane. The usual spherical fullerenes have 12 pentagons; elliptic fullerenes, 6; and toroidal and Klein-bottle fullerenes, none. Klein-bottle and elliptic fullerenes are the antipodal quotients of centrosymmetric toroidal and spherical fullerenes, respectively. Extensions to infinite systems (plane fullerenes, cylindrical fullerenes, and space fullerenes) are indicated. Eigenvalue spectra of all four classes of finite fullerenes, are reviewed. Leapfrog fullerenes have equal numbers of positive and negative eigenvalues, with 0, 0, 2, or 4 eigenvalues zero for spherical, elliptic, Klein-bottle, and toroidal cases, respectively.

INTRODUCTION

The discovery of the fullerene molecules and related forms of carbon such as nanotubes has generated an explosion of activity in chemistry, physics, and materials science, which is amply documented elsewhere.[1−4] In chemistry, the "classical" definition is that a fullerene is an all-carbon molecule in which the atoms are arranged on a pseudospherical framework made up entirely of pentagons and hexagons, which therefore necessarily includes exactly 12 pentagonal rings. "Nonclassical" extensions to include rings of other sizes have been considered (e.g. ref 5) and may be competitive in energy with the classical fullerenes in some ranges of nuclearity (e.g. ref 6). The present paper is concerned with a generalization in a different direction: what fullerenes are possible if a fullerene is a finite trivalent map with only 5- and 6-gonal faces embedded in any surface (i.e. a 2-manifold in the mathematical sense)? This seemingly much larger concept leads to a small number of well-defined extensions to the class of spherical fullerenes, actually three in number. Of these only the toroidal fullerenes are likely to have direct experimental relevance (indeed observation of a toroidal "fullerene crop circle" has already been reported[7]), but all three extensions are useful in placing physical fullerenes in a wider mathematical context and are considered in this light here. A more mathematical treatment of the concept of the extended fullerenes and their further generalization to higher dimensional spaces is given elsewhere.[8]

CLASSIFICATION OF FINITE FULLERENES

Define a fullerene in the wider sense as a finite, trivalent map on a surface and consisting of only 5-gonal and 6-gonal faces. Each such object has n vertices, e edges, and f faces of which f_5 are pentagons and f_6 hexagons. Infinite analogues of fullerenes will be considered in a later section.

The Euler characteristic χ is defined as the number

$$\chi = n - e + f \tag{1}$$

which for a trivalent graph (hence having $2e = 3n$) made up of pentagons and hexagons (and hence $2e = 5f_5 + 6f_6$) is

$$\chi = f_5/6 \tag{2}$$

For a surface in which a fullerene in this extended sense can be embedded, the number χ is therefore a nonnegative integer. In the well-known classification of compact 2-manifolds, any such manifold is homeomorphic to a sphere with g handles (if orientable) or to a sphere with g cross-caps (if nonorientable). [Handles are made from cylinders and cross-caps from twisted cylinders (see ref 9 for details).] Hence, the Euler characteristic χ for a closed surface (i.e. a surface without a boundary) is also given by

$$\begin{aligned} \chi &= 2\,(1 - g) \qquad \{\text{(for an orientable surface)} \\ &= 2 - g \qquad \{\text{(for a nonorientable surface)} \end{aligned} \tag{3}$$

The cases compatible with nonnegative integral solutions for χ are thus exactly four in number. The only surfaces admitting finite fullerene maps in the sense of our definition are therefore as follows: S^2 (the sphere, orientable with $g = 0$), T^2 (the torus, orientable with $g = 1$), K^2 (the Klein bottle, nonorientable with $g = 2$), and P^2 (the real projective plane, also called the elliptic plane, nonorientable with $g = 1$). All embeddings are *2-cell*, meaning that each face is homeomorphic to an open disk. An immediate consequence of Euler's formula is that fullerenes on S^2, T^2, K^2, and P^2 have exactly 12, 0, 0, and 6 pentagons, respectively. The four possible classes of fullerenes are therefore *spherical*, *toroidal*, *Klein-bottle*, and *elliptic*. No other surfaces are compatible with the definition. Toroidal and Klein-bottle fullerenes may also be called toroidal and Klein-bottle *polyhexes*[10,11] since they include no pentagons.

Maps on S^2 can be drawn as the usual Schlegel diagrams, and maps on T^2, K^2, and P^2 by identifying opposite edges of

* To whom correspondence should be addressed. E-mail: deza@dmi.ens.fr; p.w.fowler@ex.ac.uk; rassat@chimene.ens.fr; k.m.rogers@ex.ac.uk.
† Laboratoire d'Informatique, Ecole Normale Supérieure.
‡ University of Exeter.
§ Department of Chemistry, Ecole Normale Supérieure.

10.1021/ci990066h CCC: $19.00
Published on Web 03/18/2000

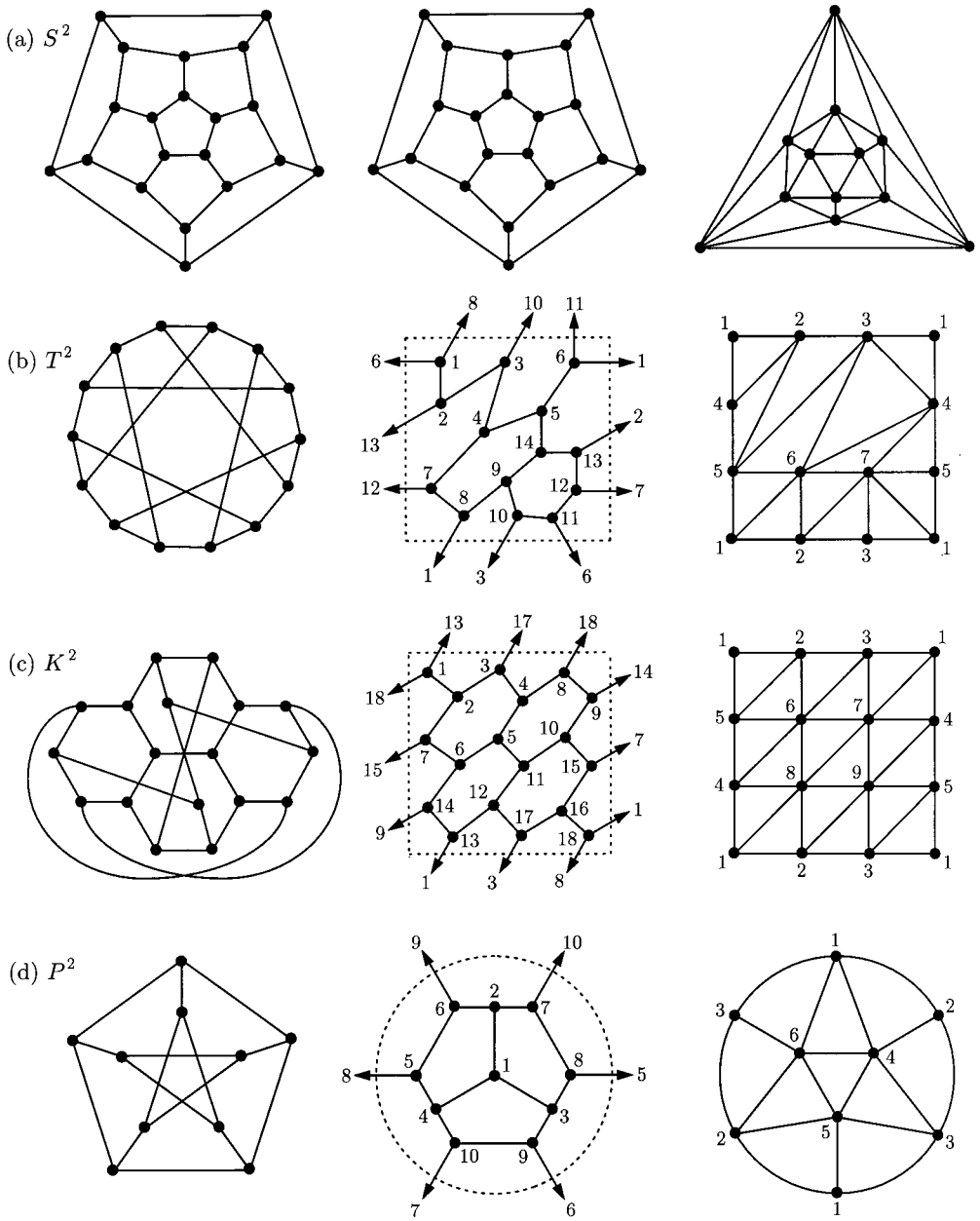

Figure 1. Smallest spherical, toroidal, Klein-bottle, and elliptic fullerenes. The first column lists the graphs drawn in the plane; the second, the map in the appropriate surface; and the third, the dual in the same surface. The examples are (a) the dodecahedron (dual icosahedron), (b) the Heawood graph (dual K_7), (c) a small Klein-bottle polyhex (dual $K_{3,3,3}$), and (d) the Petersen graph (dual K_6).

a fundamental parallelogram with appropriate orientation. Maps on P^2 are more usually drawn inside a circular frame where antipodal boundary points are to be identified. Figure 1 shows examples of small fullerenes from the four classes, drawn as the graph, the map, and its dual triangulation in the appropriate surface. We remark that the Petersen and Heawood graphs which appear naturally here are actually the 5- and 6-cages (a *k*-cage is a trivalent graph of smallest cycle size *k* with the largest possible number of edges); their duals in P^2 and T^2, K_6 and K_7, realize the chromatic number of the corresponding surfaces.

Spherical and toroidal fullerenes have an extensive chemical literature, and Klein-bottle polyhexes have been considered in several papers.[11−13] The review chapter by Klein and Zhu[13] in particular, introduces many of the relevant concepts from surface topology to a chemical context. Elliptic fullerenes have appeared so far only in ref 8, but turn out to be related in a simple way to a subclass of the known spherical fullerenes, as shown later.

Spherical Fullerenes. It has been proved that at least one spherical fullerene with n vertices (modeling a carbon molecule C_n) exists for all even n with $n \geq 20$ except for the case $n = 22$.[14] Each fullerene polyhedron has $f_5 = 12$ pentagons and $f_6 = n/2 - 10$ hexagons. Chemical interest centers on isolated-pentagon fullerenes, which can be constructed for $n = 60$ and for all even values of $n \geq 70$ (thus with $f_6 = 20$ and $f_6 \geq 25$). Aspects of the systematics of spherical fullerenes including chemical results are summarized in, e.g., ref 2.

Toroidal and Klein-Bottle Fullerenes. T^2- and K^2-polyhexes are related to the hexagonal tessellation of the graphite sheet in a straightforward way. The underlying surfaces are quotients of the Euclidean plane R^2 under groups of isometries generated by two translations (for T^2) or one

Table 1. Enumeration of Toroidal Polyhexes[a]

f_6	1	2	3	4	5	6	7	8	9	10	11	12	13	14
regular	1	1	2	3	2	3	3	5	4	4	3	8	4	5
polyhedral	–	–	–	–	–	–	1	1	2	1	1	4	2	2
fully symmetric	1	–	1	1	–	–	1	–	1	–	–	1	1	–
	(1, 0)	–	(1, 1)	(2, 0)	–	–	(2, 1)	–	(3, 0)	–	–	(2, 2)	(3, 1)	–

[a] f_6 is the number of hexagonal faces. The count of regular polyhexes is for 2-cell embeddings of trivalent maps with all faces hexagonal. Polyhedral polyhexes are those in which the intersection of any two faces is either an edge or is empty. The final rows give the counts and canonical lattice-vector parameters for the restricted class of regular polyhexes of maximal automorphism group.

translation and one glide reflection (for K^2). Each point of T^2 and K^2 corresponds to an orbit of the generating group. For completeness, we note that the groups generated by a single translation or a single glide reflection respectively give as quotients the cylinder and the twisted cylinder (the Möbius surface). Construction and enumeration of polyhexes can therefore be envisaged as a process of cutting parallelograms out of the graphite plane and gluing their edges according to the rules implied in Figure 1.

Some confusion exists in the mathematical and chemical literature of toroidal polyhexes. Negami,[15] Altschuler,[16] and other topological graph theorists define regular 3-valent maps on the torus to mean 2-cell embeddings with all faces hexagonal, without further qualification. Errera,[17] Brahana,[18] Coxeter and Moser,[19] and others working in a group theoretical tradition use the same term in a more restricted sense of polyhexes with automorphism groups G of the maximal possible order $|Aut(G)|$, in other words, those that realize the equality in the analogue of the Weinberg bound $|Aut(G)| \leq 4e(G)$ ($=12f_6$ for a polyhex). These regular maps are called *fully symmetric* by Nakamoto in his thesis.[20] All such fully symmetric graph embeddings are (on S^2) the five Platonic polyhedra, (on P^2) six graphs that include the Petersen graph and its dual, (on K^2) no graphs at all,[20] and (on T^2) the polyhexes that arise from an analogue of the Goldberg/Coxeter construction of icosahedral S^2-fullerene polyhedra.[21,22]

Here we consider only *polyhedral* polyhexes, i.e., those without loops or multiple edges and where the intersection of any two faces is either one edge or is empty. The dual of a toroidal polyhedral polyhex is a triangulation of the torus. To illustrate the relationship of the various definitions, we give the counts for small cases in Table 1, using data extracted from the papers of Negami[15] and Altschuler.[16] The tabulations given by Kirby[10,12] include some nonpolyhedral cases.

In Negami's construction, a three-parameter code[15] represents any toroidal polyhex (or, equivalently, any 6-regular triangulation of T^2) as a tessellation of the hexagonal lattice. Each graph of this type is denoted $T(p,q,r)$, with integer parameters p, q, and r, where p is the length of a geodesic cycle of edge-sharing hexagons, r is the number of such cycles, and q is an offset.

Polyhex maps on T^2 are constructible for all values $f_6 \geq 3$, $n \geq 6$.[23] At least one *polyhedral* toroidal polyhex exists for all even numbers of vertices $n \geq 14$. The unique polyhedral toroidal fullerene at $n = 14$ is a realization of the Heawood graph. It has indices (2,1) in the Goldberg/Coxeter construction and is the dual of K_7, the complete graph on seven vertices, which itself realizes the 7-color map on the torus. This map and its dual are shown in Figure 1.

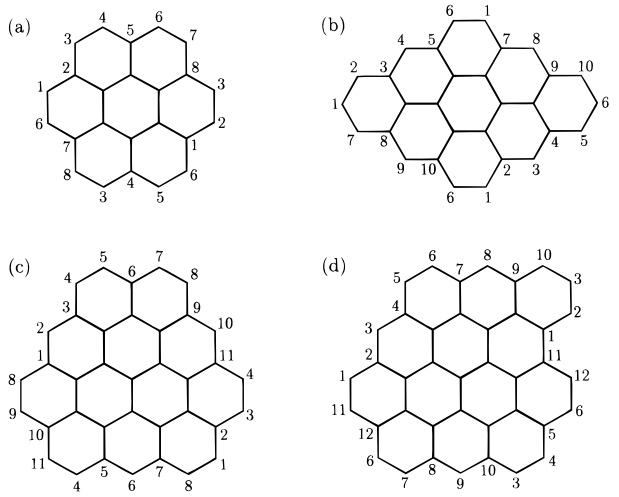

Figure 2. Examples of small polyhedral toroidal polyhexes presented as benzenoids with glued vertices (indicated on the periphery). These are the polyhexes with Coxeter/Goldberg codes (2,1), (3,0), (2,2), (3,1). The map (2,1) is the Heawood graph, which is drawn in two different presentations in Figure 1.

A different presentation of this and the next three toroidal polyhexes obtainable by the Goldberg/Coxeter construction are illustrated in Figure 2.

A description of Klein-bottle polyhexes can be developed along similar lines.[20,24] Each toroidal graph $T(p, 0, r)$ can be used to obtain two Klein-bottle 6-regular triangulations (and hence, by dualization, fullerenes), the *handle* and *cross-cap* types $K_h(p, r)$ and $K_c(p, r)$, respectively. The torus is cut along a geodesic of length p. Then the *handle* construction amounts to identification of opposite sides of the resulting parallelogram with reversed direction. In the *cross-cap* construction, the opposite sides are each converted to cross-caps, with slightly different rules for odd and even p. See also ref 25 for pictures of the two types of Klein bottle. Polyhex maps on K^2 are constructible for all values $f_6 \geq 3$, $n \geq 6$.[23] The unique smallest *polyhedral* Klein-bottle polyhex has 18 vertices (9 hexagonal faces) and is the dual of the tripartite $K_{3,3,3}$; the graph, the map, and its dual are shown in Figure 1.

It will turn out to be useful for calculation of spectra later that each Klein-bottle polyhex graph, whether of handle or cross-cap type, has a double cover among the centrosymmetric toroidal polyhexes. In contrast with a T^2-polyhex, a polyhex on K^2 may or may not be bipartite, i.e., spanned by two disjoint sets of vertices, black and white, such that every white vertex is surrounded by black and *vice versa*.

Elliptic Fullerenes. Torus and Klein-bottle arise as quotient spaces, as described above, and this leads to a construction of the possible polyhex maps. Within the same framework the real projective plane arises as a quotient space

of the sphere, the required group being C_i. The real projective plane (also known as the elliptic plane) is obtained by identifying antipodal points of the spherical surface; in other words, it is the *antipodal quotient* of the sphere. P^2 is the simplest compact nonorientable surface in the sense that it can be obtained from the sphere by adding just one cross-cap.

Clearly, this construction can be carried over to maps: the antipodal quotient of a centrosymmetric map on the sphere has vertices, edges, and faces obtained by identifying antipodal vertices, edges, and faces, thereby halving the number of each type of structural component. For example, the antipodal quotient of the icosahedron is K_6, the complete graph on 6 vertices, and that of the dodecahedron is the Petersen graph, famous as a counterexample to many theorems. The Petersen graph is not planar, but it is called *projective-planar* in the sense that it can be embedded without edge crossings in the real projective plane.

In this terminology, our definition of elliptic fullerenes amounts to selection of polyhedral projective-planar trivalent maps with only 5- and 6-gonal faces. As noted above, $f_5 = 6$ for these maps. Thus, the Petersen graph is an elliptic fullerene (the smallest). Maps on P^2 with $f_5 = 6$ are constructible for $f_6 = 0$ and for all values $f_6 \geq 3$.[23] Not all of these are polyhedral. In general the elliptic fullerenes are exactly the antipodal quotients of the centrosymmetric spherical fullerenes. From any centrosymmetric fullerene it is possible to construct a unique elliptic fullerene by identifying antipodal vertices, and from any elliptic fullerene it is possible to reconstruct uniquely the original centrosymmetric fullerene.

Thus, the problem of enumeration and construction of elliptic fullerenes reduces simply to that for centrosymmetric conventional spherical fullerenes. The point symmetry groups that contain the inversion operation are C_i, C_{nh} (n even), D_{nh} (n even), D_{nd} (n odd), T_h, O_h, and I_h. A spherical fullerene may belong to one of 28 point groups[2] of which 8 appear in the previous list: C_i, C_{2h}, D_{2h}, D_{6h}, D_{3d}, D_{5d}, T_h, and I_h. Clearly, a fullerene C_n can be centrosymmetric only if n is divisible by 4 as f_6 must be even, but also $f_6 = n/2 - 10$. After the minimal case $n = 20$, it turns out that there are no centrosymmetric fullerenes at $n = 24$ and $n = 28$ and unique examples at 32 (D_{3d}) and 36 (D_{6h}). Complete enumerations of general centrosymmetric fullerenes on up to 100 atoms and of isolated pentagon centrosymmetric fullerenes of up to 140 atoms taken from the Fullerene Atlas[2] are given in Tables 2 and 3. All generate elliptic fullerenes by antipodal identification.

It seems likely that at least one centrosymmetric fullerene exists for all doubly even values of $n \geq 32$ and at least one centrosymmetric fullerene with isolated pentagons for every doubly even $n \geq 92$, though we are not aware of a proof. For four of the eight point groups, explicit conditions are known for the existence of a fullerene of the given symmetry at a given n: I_h fullerenes C_n exist for all distinct solutions (i, j) of $n = 20(i^2 + ij + j^2)$ with either $i = j$ or $j = 0$, and similar but more complicated conditions are known for T_h, D_{5d}, and D_{6h} fullerenes.[26]

Table 2. Centrosymmetric Fullerenes C_n ($20 \leq n \leq 100$) with and without Pentagon Adjacencies[a]

n	C_i	C_{2h}	D_{2h}	D_{6h}	D_{3d}	D_{5d}	T_h	I_h	total
20	0	0	0	0	0	0	0	1	1
24	0	0	0	0	0	0	0	0	0
28	0	0	0	0	0	0	0	0	0
32	0	0	0	0	1	0	0	0	1
36	0	0	0	1	0	0	0	0	1
40	0	0	1	0	0	2	0	0	3
44	0	0	0	0	3	0	0	0	3
48	0	1	2	0	0	0	0	0	3
52	0	1	2	0	0	0	0	0	3
56	1	2	1	0	2	0	0	0	6
60	0	4	1	2	0	1	0	1	9
64	2	4	1	0	0	0	0	0	7
68	0	7	2	0	3	0	0	0	12
72	3	7	5	0	0	0	0	0	15
76	2	11	0	0	0	0	0	0	13
80	5	16	0	0	2	2	0	1	26
84	9	4	6	2	1	0	0	0	22
88	10	16	5	0	0	0	0	0	31
92	12	13	4	0	5	0	1	0	35
96	20	16	3	2	1	0	0	0	42
100	14	28	2	0	0	2	0	0	46
total	78	130	35	7	18	7	1	3	279

[a] Each is the parent of an elliptic P^2-fullerene.

Table 3. Centrosymmetric Fullerenes C_n ($60 \leq n \leq 140$) with Isolated Pentagons[a]

n	C_i	C_{2h}	D_{2h}	D_{6h}	D_{3d}	D_{5d}	T_h	I_h	total
60	0	0	0	0	0	0	0	1	1
72	0	0	0	0	0	0	0	0	0
76	0	0	0	0	0	0	0	0	0
80	0	0	0	0	0	1	0	1	2
84	0	0	0	1	1	0	0	0	2
88	0	0	0	0	0	0	0	0	0
92	0	0	1	0	0	0	0	0	1
96	0	0	1	1	1	0	0	0	3
100	0	0	0	0	0	1	0	0	1
104	0	0	2	0	1	0	0	0	3
108	0	3	1	1	1	0	0	0	6
112	0	2	1	0	0	0	0	0	3
116	0	2	1	0	0	0	1	0	4
120	1	5	3	0	0	3	0	0	12
124	1	5	1	0	0	0	0	0	7
128	3	4	0	0	2	0	0	0	9
132	0	10	2	1	5	0	0	0	18
136	4	12	3	0	0	0	0	0	19
140	8	7	0	0	0	1	0	0	16
total	17	50	16	4	11	6	1	2	107

[a] Each is the parent of an elliptic P^2-fullerene.

SOME INFINITE ANALOGUES OF FULLERENES

All the fullerenes considered so far are finite and are actually trivalent tilings with (combinatorial) pentagons and hexagons of particular surfaces. If instead of S^2, T^2, K^2, or P^2, we consider tilings of the Euclidean plane R^2, a natural definition is obtained for an *infinite* fullerene analogue. Namely, a *plane fullerene* is a trivalent tiling of R^2 by combinatorial pentagons and hexagons. Deza and Shtogrin[8] proved that the number of pentagons in a planar fullerene is at most 6. This follows from an old result of Alexandrov.[27] It is easy to see that the plane fullerenes with $f_5 = 0$ (the graphite sheet) and $f_5 = 1$ (a pentagonal cone) are unique. However, there is an infinity of possibilities for $2 \leq f_5 \leq 6$. Restriction to bounded tile size eliminates pathological possibilities such as an infinite tube capped by a hemi-dodecahedron. The restriction to trivalence is also a powerful one: by allowing also four-valent vertices, for example, R^2 could be partitioned into pentagons in a tiling with vertices

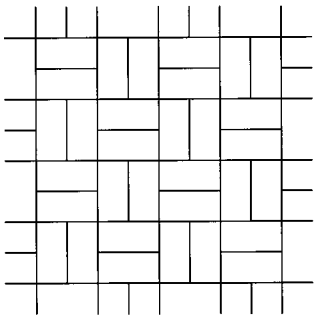

Figure 3. Tiling of the plane with combinatorial pentagons alone in which all vertices are of degree 3 or 4.

of degrees 3 and 4 (Figure 3), which would not be a fullerene in our sense. Another such example but with congruent convex pentagons is the Cairo tiling [the dual of the Archimedean tiling $(3.4.3^2.4)$].

Other infinite fullerenes would be given by trivalent tilings with pentagons and hexagons of the cylinder, semiinfinite cylinder, twisted cylinder, etc. Such a tiling on the cylinder is a polyhex and is the infinite open nanotube.

The tiling description also leads naturally to definition of a *space fullerene* as a four-valent tiling of R^3, where each cell is a conventional fullerene polyhedron. It turns out that those space fullerenes where the cells have no adjacent *hexagons* [C_{20}, C_{24}, C_{26}, C_{28} (T_d)] are of special interest, though others have been constructed.[8] These space fullerenes occur in chemistry and physics as the "dodecahedral family of hydrates"[28] (clathrates) and their duals as "tetrahedrally close-packed phases" (tcp) or generalized Frank−Kasper phases.[29−31] If the inventory of cells is extended to the C_{22} "near fullerene" (the edge-truncated dodecahedron with 1 square, 10 pentagonal, and two hexagonal faces), other phases can be represented, e.g., Hume-Rothery's phase γ has C_{20}:C_{22}:C_{26} in the proportion 2:2:3.[31]

In the hydrate structures the "vertices" are water molecules with two donor and two acceptor hydrogen bonds. Each space fullerene gives rise to a hypothetical silicate structure if every vertex is replaced by an SiO_4 tetrahedron, or a hypothetical carbon allotrope if every vertex is replaced by a single carbon atom. Combinations tabulated by Wells[28] can be represented in an obvious "chemical" fullerene notation as $(C_{20})(C_{24})_3$, $(C_{20})_2(T_d\ C_{28})$, $(C_{20})_3(C_{24})_2(C_{26})_2$ and $(C_{20})_5(C_{24})_8(C_{26})_2$. The first of these is illustrated in Figure 4. A new structure consisting of C_{20}-, C_{24}- and C_{36} (D_{6h})-cells is given by Deza and Shtogrin.[8] Four-valent honeycombs with fullerene and similar cells also figure in modern conjectured solutions to the Kelvin problem of finding a partition of three-dimensional space into cells of equal volume and minimal surface area (see also other papers in the volume containing refs 30 and 32). The best foam found so far[32] is the dual of the A15 Frank−Kasper structure and is a metric variation of $(C_{20})(C_{24})_3$.

Generalizing further, the vertices could be replaced by larger entities such as tetrahedral C_{28} fullerenes bonded through their four apical atoms to make a super-fullerene lattice. The 3D tilings open up a number of questions of enumeration, characterization, and spectral structure, to answer which will require further work.

We note that plane fullerenes can be seen as infinite fullerene polyhedra, and space fullerenes, as an infinite

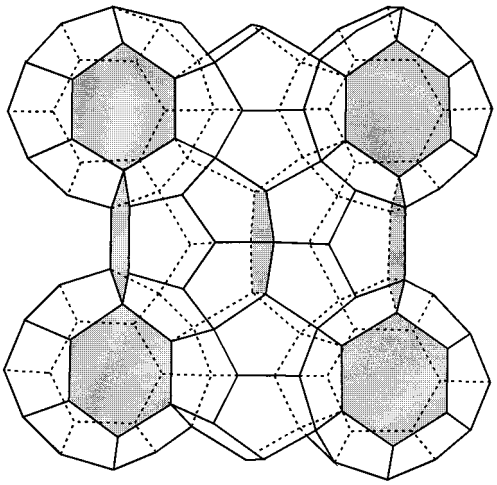

Figure 4. Smallest space fullerene: an assembly of 20- and 24-vertex spherical fullerenes in ratio 2:6 (see Wells[28]). Different metric variations of this structure appear as a clathrate and as the best Kelvin foam. Its dual is A15, the structure of β-tungsten and Cr_3Si.

analogue of a four-dimensional fullerene. A four-dimensional fullerene (a *polytopal 4-fullerene* in the language of ref 8) is therefore a simple 4-polytope having only five- and six-sided two-faces. Clearly, all cells of such structures are fullerenes.

EIGENVALUE PROPERTIES

A first indication of the qualitative π-electronic structure to be expected of the new frameworks as hypothetical forms of carbon can be gained from Hückel theory, for which a prerequisite is a knowledge of the adjacency properties. For orientable surfaces there is a clear link between the spectrum of the adjacency matrix of the map and the π-orbital energies of its realization as a carbon framework. In the simplest Hückel model, each eigenvalue λ of the matrix corresponds to an orbital of energy $\alpha + \lambda\beta$, where α is the Coulomb parameter, assumed the same for every site, and β the resonance parameter, assumed equal for all bonds. For nonorientable surfaces such as K^2 and P^2 this correspondence is lost because the intrinsic twist in the surface introduces a phase discontinuity in the π-basis. The relevant eigenvalues are then those of a weighted adjacency matrix, as will be discussed below.

It should be remembered that π energy is only one contribution to the total energy, and in real spherical fullerenes it is dominated by the strain in the σ system, which leads for example to the observation that stable fullerenes are not necessarily those of maximal Hückel energy.[2] As real carbon systems, T^2-fullerenes are highly strained and are unlikely to be realized unless for very large values of n; the toroidal nanotube reported by Liu et al.[7] has a diameter of 330−500 nm, implying many thousands of atoms. Chemical systems based on K^2- and P^2-polyhexes are less plausible, as these systems involve self-intersection. Klein[11] suggests a mode of interlocking of graphitic planes that may minimize the very considerable energetic costs, but the interest of these systems is likely to remain purely mathematical for a long while to come.

(a) Orientable Fullerenes. (1) *S^2-Fullerenes.* The situation for the usual spherical fullerenes has been well-explored. Adjacency matrices of spherical fullerenes have

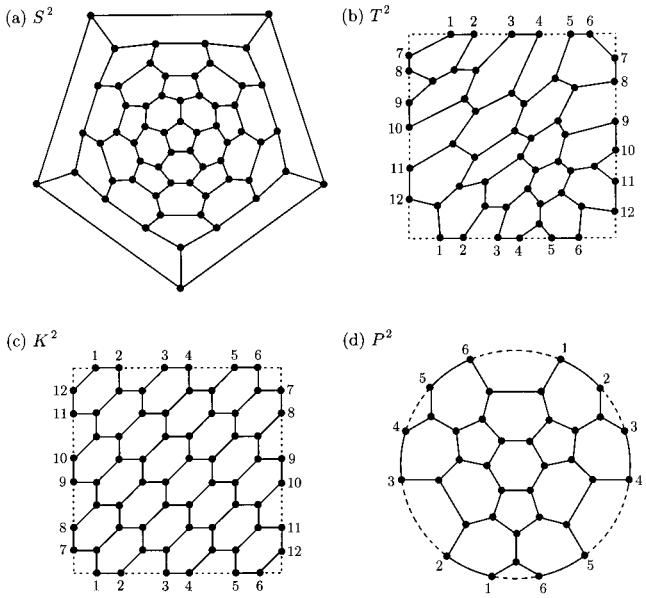

Figure 5. Leapfrogs of the smallest polyhedral fullerenes on the surfaces S^2, T^2, K^2, and P^2.

typically more positive than negative eigenvalues, correlating with their chemical behavior as electron-deficient π-systems. Only occasional examples with more negative than positive eigenvalues are known.[33] A special subclass with equal numbers of positive and negative eigenvalues, and therefore an "ideal" π-structure, is formed by the *leapfrog* fullerenes C_n, each constructed by omnicapping and then dualizing a smaller S^2-fullerene $C_{n/3}$.[34] Other spherical fullerenes with exactly $n/2$ positive eigenvalues are possible, but are rare compared to the leapfrogs.[2]

Leapfrogging can be carried out on any surface, with characteristic implications for the eigenvalue spectrum. As an illustration of the leapfrog construction on nonspherical surfaces, the leapfrogs of the smallest spherical, toroidal, Klein-bottle, and elliptic fullerenes are given in Figure 5. The striking spectral regularities from the leapfrog transformation can be rationalized in terms of the way that relationships between structural components in a parent carry over to the leapfrog map. Each face of the parent gives rise to a congruent but rotated face in the leapfrog; these *Clar* faces are disjoint and exhaust the vertices of the leapfrog. All faces of the leapfrog outside the Clar set are hexagons centered on the sites of the parent vertices. Each edge of the parent gives rise to a rotated edge in the leapfrog; these *Fries* edges are again disjoint and account for one-third of the edges of the leapfrog and all of its vertices. The Fries edges radiate from the Clar faces, so that every edge of the leapfrog is either Fries or *Clar* (i.e., an edge of a Clar face).

A consistent Kekulé structure can be built for leapfrog fullerenes on any of the four surfaces by placing formal double bonds on the Fries edges and formal single bonds on the Clar edges. This *Fries* structure has the maximum possible number of simultaneous benzenoid hexagons, one for each vertex of the parent, giving an ideal localized electronic structure for the neutral carbon cage C_n. A delocalized version of the argument uses considerations based on the Rayleigh inequality for the distinct basis sets consisting of all bonding (in-phase) or all antibonding (out-of-phase) combinations along Fries edges[35] and shows that S^2-leapfrog fullerenes have *no* zeros and hence closed shells as neutral molecules.

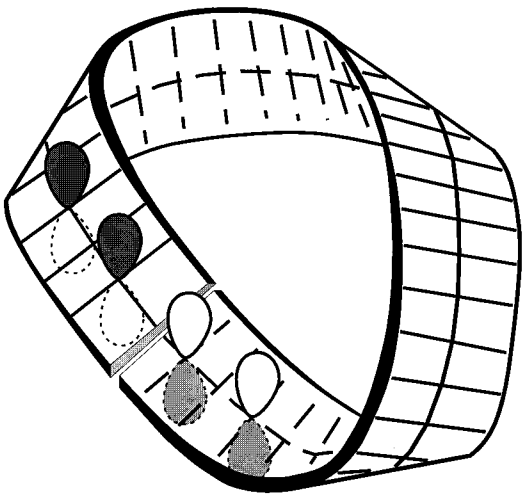

Figure 6. Construction of a nonorientable surface such as a Möbius strip by twisting and gluing a planar system brings together p orbitals of opposite phase across the seam of the twist.

A second localized structure places a sextet of π-electrons on every Clar face and a single bond on every Fries edge; this is a formal model of the electronic structure of the anionic system $C_n^{f_5-}$ bearing an excess of f_5 electrons. This too has its counterpart in delocalized molecular-orbital theory, where the extra 12 electrons of a leapfrog S^2-fullerene anion C_n^{12-} occupy low-lying antibonding orbitals of translational and rotational symmetry.[36]

(2) *T^2-Fullerenes.* Eigenvalue spectra of toroidal polyhexes have been studied in some detail. Kirby et al.[10] give an explicit formula for calculation of the set of eigenvalues in terms of canonical lattice-vector parameters. T^2-polyhexes have symmetric spectra (with both $+\lambda$ and $-\lambda$ occurring for every eigenvalue λ), as they are bipartite graphs, and all eigenvalues λ except ± 3 and ± 1 have even multiplicity. The special eigenvalue $\lambda = 0$ is governed by a simple pattern: exactly those toroidal polyhedral polyhexes that are leapfrogs have open shells, with four zero eigenvalues at positions $n/2 - 1$, $n/2$, $n/2 + 1$, and $n/2 + 2$ in the spectrum.[37] The spectra of toroidal polyhexes are also intimately related to those of spherical triangle and hexagon polyhedra and explain endospectral regularities in the latter series.[38]

(b) Nonorientable Fullerenes. As warned earlier, there is a subtlety in the application of Hückel theory to frameworks embedded in nonorientable surfaces. The problem arises as follows. The π-basis consists of a p function on every participating carbon atom, directed along the normal to the surface, and Hückel energies are obtained by diagonalizing a Hamiltonian matrix whose entries are pairwise integrals of these (vectorlike) functions. Under the usual assumptions, only functions on nearest neighbors are involved. For an orientable surface, neglecting curvature, neighboring normals are parallel and the integrals are therefore proportional to entries in the adjacency matrix. However, for a nonorientable surface made by gluing edges of a patch together with a twist, p functions neighboring across the join become antiparallel and for such pairs the integral is reversed in sign (see Figure 6).

A standard chemical example occurs in the theory of Möbius transition states for pericyclic processes where

eigenvalues for cycles with one phase interuption are found by diagonalizing a weighted adjacency matrix that has an entry -1 for one link and $+1$ for all others. The spectrum of the Möbius cycle can be found by rotation of the usual geometric construction for untwisted cycles.[39] In the present case, an analogous procedure can be adopted: to construct the dimensionless Hückel Hamiltonian matrix, **H**, take the adjacency matrix **A** of the graph and multiply by -1 all entries for edges that cross a twisted boundary (in the case of K^2) or cross the circular boundary (in the case of P^2). Signs for any edges terminating at or lying within a boundary can be decided by making small shifts to bring their vertices inside the boundary.

(1) *K^2-Fullerenes.* Some calculations of eigenvalues of unweighted adjacency matrices of Klein-bottle polyhexes have been reported[40] and compared with those of toroidal polyhexes, but a general picture of the spectra for these systems has not been given.

The Klein-bottle surface can be obtained by identifying diametrically opposite points of the torus, i.e., by collapsing each point and its antipode.[41] The point groups available to the covering torus are at most the centrosymmetric subgroups of $D_{\infty h}$, i.e., D_{nh} and C_{nh} (n even), D_{nd} and S_{2n} (n odd), C_i, though, as with spherical fullerenes, some of the lower groups may not be realisable. Hence, each K^2-polyhex on n vertices is doubly covered by a centrosymmetric T^2-polyhex on $2n$ vertices and is therefore a *divisor*[42] of the larger graph. By a centrosymmetric graph, we mean, as usual, a graph that has a centrosymmetric setting on the appropriate surface, i.e., has centrosymmetric maximal symmetry. The weighted K^2-polyhex represented by the **H** matrix is the co-divisor. Any given eigenvector of the adjacency matrix of the larger T^2-polyhex therefore corresponds to an eigenvalue in the spectrum of **A** (**H**) of the smaller K^2-graph if the antipodal vertices carry equal (opposite) coefficients. Eigenvectors of the covering graph can always be projected to display this *gerade/ungerade* symmetry. Figure 7 shows the construction of double covers for two small Klein-bottle polyhexes. Given a K^2-polyhex, the double cover can always be constructed and reduced to canonical form and its spectrum partitioned into that of **A** (K^2) and **H** (K^2).

A simple pattern can be observed in the partitioned spectra. Consider a given eigenvector $|\lambda\rangle$ with eigenvalue λ in the toroidal double cover. As the covering T^2-polyhex is bipartite, a change of sign of the coefficient on every vertex of one partite set generates an eigenvector $|-\lambda\rangle$ of eigenvalue $-\lambda$. On collapsing pairs of covering vertices, $|+\lambda\rangle$ will generate an eigenvector of either **A** or **H**, as will $|-\lambda\rangle$. Two different situations are possible:

(i) *The K^2-polyhex itself is bipartite*: $|+\lambda\rangle$ and $|-\lambda\rangle$ yield eigenvectors with eigenvalues belonging to one and the same subspectrum, either the spectrum of **A** or the spectrum of **H**. For example, in this case, the **A** spectrum always contains $\lambda = 3$ and $\lambda = -3$, whereas the **H** spectrum contains neither.

(ii) *The K^2-polyhex itself is nonbipartite*: $|+\lambda\rangle$ and $|-\lambda\rangle$ yield eigenvectors with eigenvalues belonging to different subspectra, one to the spectrum of **A** and one to that of **H**. As a consequence, the two subspectra are exact reversals of one another. In particular, the **A** spectrum always contains $\lambda = +3$ and the **H** spectrum $\lambda = -3$.

The origin of properties i and ii is readily explained. Take the patch of hexagons that generates the K^2-polyhex, and

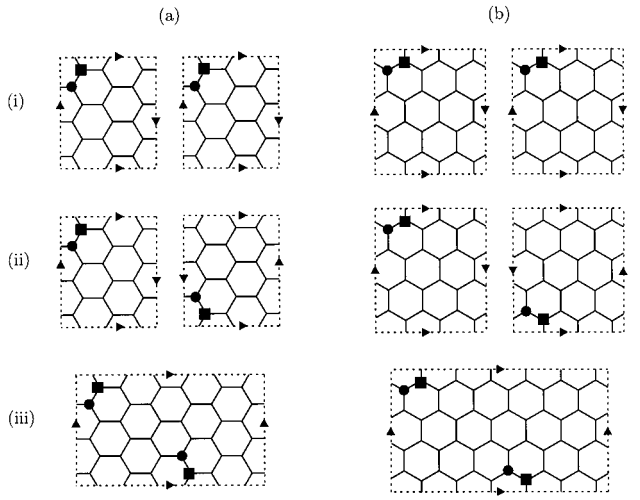

Figure 7. Construction of toroidal double covers of Klein-bottle polyhexes: (a) shows a bipartite K^2-polyhex on 18 vertices which is covered by a centrosymmetric D_{3d} torus on 36 vertices; (b) shows a nonbipartite K^2-polyhex on 24 vertices, covered by a 48-vertex, centrosymmetric D_{6h} torus. The steps in the construction are as follows: (i) copy the Klein-bottle polyhex by a simple translation; (ii) flip the second copy by 180° about the translation vector; (iii) fuse the two copies. The arrows indicate edge identifications, and members of a pair of covering vertices are marked with the same symbol (filled circle or square). Note that in case a, the two covering vertices are to be found in the same partite set on the torus, whereas in case b they are not.

color its vertices alternately black and white. Further, take an eigenvector $|\lambda\rangle$ of the covering torus that yields a vector of the same eigenvalue for **A**. $|\lambda\rangle$ will have the property that any one pair of antipodal vertices on the torus share a coefficient. Now attach to each vertex of the patch the common value of the coefficient from its covering pair, to produce a self-consistent eigenvector of **A**, $|\lambda(\mathbf{A})\rangle$. If the K^2-polyhex is bipartite (case i), reversal of the coefficients of all black vertices of the patch gives another self-consistent eigenvector of **A**, $|-\lambda(\mathbf{A})\rangle$. However, if the K^2-polyhex is nonbipartite (case ii), then when the patch is joined up to make the Klein-bottle each edge of the graph that crosses the twisted boundary will join vertices of like color, since it is these edges that destroy the alternating pattern of the planar patch. In such a case, weighting these edges by -1 and simultaneously reversing all coefficients on the vertices of one color gives an eigenvector of **H** with eigenvalue $-\lambda$, i.e., $|-\lambda(\mathbf{H})\rangle$, QED.

A leapfrog rule can be derived for K^2-polyhexes. Consider a patch cut from the hexagonal tessellation of the plane, such that it can be rolled up to give both leapfrog T^2- and K^2-polyhexes. This possibility implies that the vertices of the patch are spanned by Clar hexagons. Figure 8 shows such a patch. When wrapped as a torus, the polyhex must have four zero-eigenvalue vectors, as it is a leapfrog. Parts c−f of Figure 8 show their explicit form. In terms of the Fries edges, both bonding and antibonding spaces each contribute two adjacency eigenvectors of zero eigenvalue. Inspection of the figure shows that different subsets of exactly two of the four survive as eigenvectors of either **A** or **H** matrices when the same polyhex is glued as a K^2-fullerene. The Rayleigh inequality arguments used in refs 35 and 43 show that, as bonding and antibonding spaces each contribute one zero in the Klein-bottle form, the two zeroes are eigenvalues $n/2$ and $n/2+1$, i.e., HOMO and LUMO of the hypothetical

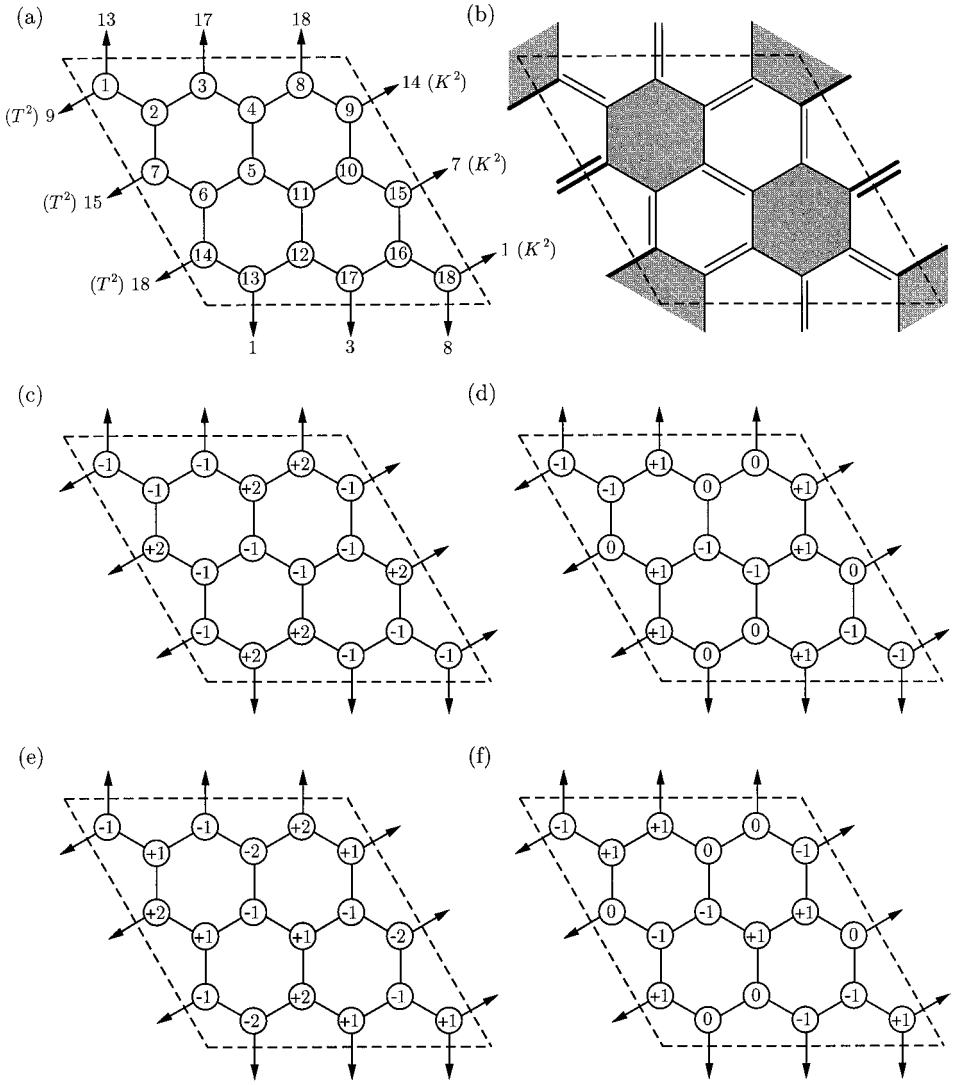

Figure 8. Origin of zero eigenvalues in toroidal and Klein-bottle leapfrog polyhexes. An 18-vertex polyhex is shown in a, numbered as for connection either as a T^2-fullerene or on K^2 with the twist occurring on gluing left and right edges of the parallelogram. This polyhex is a leapfrog, as shown in b, where shading identifies Clar faces and a double bond a Fries edge. Edges crossing the seam of the twist and therefore to be weighted by −1 in the Hückel problem on K^2 are in bold. When the polyhex is connected on T^2 all four vectors c−f represent eigenvectors of **A** with zero eigenvalue. When it is connected on K^2, c and e are zero-eigenvalue eigenvectors for **A**, and d and f are zero-eigenvalue eigenvectors for **H**, the weighted adjacency matrix. Details of the construction of c−f from local bonds and antibonds on Fries edges are given in ref 43.

neutral carbon framework with this topology. The general chemical conclusion is that *all leapfrog K^2-polyhexes, whether treated as weighted or unweighted Hückel problems, have open shells, with two electrons in two nonbonding π orbitals*.

A final feature of the leapfrog transformation is illustrated by Figure 9, where the graphs of the 18-vertex K^2-fullerene, its leapfrog and double leapfrog are superimposed. Leapfrogging switches the character of the graph from bipartite to nonbipartite and back again. This is a result of a switch in parity of geodesic cycles, even though all faces remain hexagonal, and is part of a more general pattern: leapfrogging a cubic graph with all faces even switches the bipartite character on the nonorientable surfaces (K^2 and P^2) but leaves it unchanged on the orientable surfaces (S^2 and T^2).

(2) *P^2-Fullerenes*. The eigenvalue spectra, both weighted and unweighted, of an elliptic fullerene are immediately available from the adjacency spectrum of its centrosymmetric parent. The eigenvalues of **A** for a P^2-fullerene are just those of the parent that correspond to gerade eigenvectors; eigenvalues of **H** correspond to ungerade eigenvectors of the parent. Together, the weighted and unweighted spectra of the P^2-fullerene sum to the spectrum of the parent, since the smaller graph is a divisor of the larger.

A simple consequence is that any P^2-fullerene derived from a leapfrog spherical parent has a properly closed shell as a neutral π system. Proof: the leapfrog parent C_n has $n/2$ positive and $n/2$ negative eigenvalues.[35] Its bonding eigenvectors span the permutation representation of the Fries edges.[34,36] This representation has character zero under inversion as all edges shift under this operation. Hence, the centrosymmetric leapfrog S^2-fullerene C_n has $n/4$ gerade and $n/4$ ungerade bonding eigenvectors. Therefore, the spectra of **A** and **H** of the derived P^2-fullerene will each have $n/4$ bonding, $n/4$ antibonding, and zero nonbonding eigenvectors, QED. As the operation that derives P^2- from S^2-fullerenes commutes with the leapfrog transformation, this argument

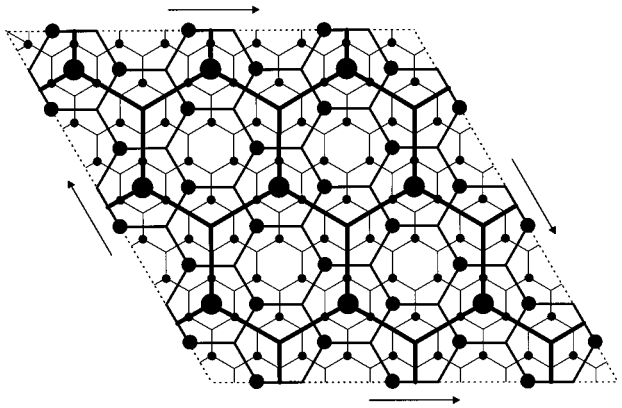

Figure 9. Multiple leapfrogs of a K^2-polyhex. The parent 18-vertex graph (thick lines) is leapfrogged to 54 and then to 162 vertices (thin lines). Only the first and third graphs are bipartite: when the patch is glued as indicated by the arrows, black vertices give a consistent partite set (filled circles) in the parent and double leapfrog but not in the single leapfrog.

proves that *leapfrog P^2-fullerenes have properly closed shells.*

CONCLUSION

This paper has explored the extension of the fullerene concept from the sphere to other surfaces, retaining trivalence and the limitation to face sizes five and six, showing that the chemical species exist within a mathematical context of a limited set of possibilities for tiling. Consideration of the extended set of surfaces also gives a context to the magic-number rules of Hückel theory, such as the leapfrog rule for closed-shell S^2-fullerenes, as it turns out that leapfrog polyhedra have distinct but predictable properties on all four surfaces. Extensions to other face sizes and more exotic surfaces will allow description of many more variants on the sphere, some of which are promising as candidates for carbon polyhedra or infinite solids.

ACKNOWLEDGMENT

The authors thank EPSRC (U.K.) and the EU TMR Network Contract FMRX-CT98-0192 "BIOFULLERENES" for financial support of this research.

REFERENCES AND NOTES

(1) Braun, T.; Schubert, A.; Maczelka, H.; Vasvári, L. *Fullerene research 1985−1993*; World Scientific: Singapore, 1995.
(2) Fowler, P. W.; Manolopoulos, D. E. *An atlas of fullerenes*, Oxford University Press: Oxford, U.K., 1995.
(3) Taylor, R., Ed., *The chemistry of fullerenes*, World Scientific: Singapore, 1995.
(4) Dresselhaus, M. S.; Dresselhaus, G.; Eklund, P. C. *Science of fullerenes and carbon nanotubes*; Academic Press: San Diego, 1996.
(5) Fowler, P. W.; Manolopoulos, D. E.; Orlandi, G.; Zerbetto, F. Energetics and isomerisation pathways of a lower fullerene: The Stone-Wales map for C_{40}. *J. Chem. Soc., Faraday Trans.* **1995**, *91*, 1421−1423.
(6) Ayuela, A.; Fowler, P. W.; Mitchell, D.; Schmidt, R.; Seifert, G.; Zerbetto, F. C_{62}: theoretical evidence for a nonclassical fullerene with a heptagonal ring. *J. Phys. Chem.* **1996**, *100*, 15634−15636.
(7) Liu, J.; Dai, H.; Hafner, J. H.; Colbert, D. T.; Smalley, R. E.; Tans, S. J.; Dekker, C. Fullerene crop circles. *Nature* **1997**, *385*, 780−781.
(8) Deza, M.; Shtogrin, M. I. Three-, four- and five-dimensional fullerenes. *SE Asian Bull. Math.* **1999**, *23*, 1−10.
(9) Gross, J. L.; Tucker, T. N. *Topological graph theory*. Wiley: New York, 1987.
(10) Kirby, E. C.; Mallion, R. B.; Pollak, P. Toroidal polyhexes. *J. Chem. Soc., Faraday Trans.* **1993**, *89*, 1945−1953.
(11) Klein, D. J. Elemental benzenoids. *J. Chem. Inf. Comput. Sci.* **1994**, *34*, 453−459.
(12) Kirby, E. C. Recent works on toroidal and other exotic fullerene structures. In *From chemical topology to 3-dimensional geometry*; Balaban, A. T., Ed.; Plenum Press: New York, 1997; Chapter 8, pp 263−296.
(13) Klein, D. J.; Zhu, H. All-conjugated carbon species. In *From chemical topology to 3-dimensional geometry*; Balaban, A. T., Ed.; Plenum Press: New York, 1997; Chapter 9, pp 297−341.
(14) Grünbaum, B.; Motzkin, T. G. The number of hexagons in and the simplicity of geodesics on certain polyhedra. *Can. J. Math.* **1963**, *15*, 744−751.
(15) Negami, S. Uniqueness and faithfulness of embedding of toroidal graphs. *Discrete Math.* **1983**, *44*, 161−180.
(16) Altshuler, A. Construction and enumeration of regular maps on the torus. *Discrete Math.* **1973**, *4*, 201−217.
(17) Errera, A. Sur les polyhedres reguliers de l'analysis situs (On the regular polyhedra of analysis situs). *Acad. R. Belg. Cl. Sci. Mem. Coll.* **1922**, *8* (2) 7, 1−17.
(18) Brahana, H. R. Regular maps on the anchor ring. *Am. J. Math.* **1926**, *48*, 225−240.
(19) Coxeter, H. S. M.; Moser, W. O. J. *Generators and relations for discrete groups*, 2nd ed.; Springer: Berlin, 1965.
(20) Nakamoto, A. Triangulations and quadrangulations of surfaces, D.Sc. thesis, Department of Mathematics, Keio University, Japan, 1996.
(21) Goldberg, M. A class of multi-symmetric polyhedra. *Tôhoku Math. J.* **1937**, *43*, 104−108.
(22) Coxeter, H. S. M. Virus macromolecules and geodesic domes. In *A spectrum of mathematics*; Butcher, J. C., Ed., Oxford University Press/ Auckland University Press: Oxford, U.K./Auckland, New Zealand, 1971; pp 98−107.
(23) Plastria, F. On the number of hexagons in cubic maps, Report BEIF/ 98, Centrum voor Bedrijfsinformatie, Vrije Universiteit Brussel, 1998.
(24) Negami, S. Classification of 6-regular Klein bottle graphs. *Res. Rep. Inf. Sci. Tokyo Inst. Technol.* **1984**, *A96*.
(25) Stillwell, J. *Classical topology and combinatorial group theory*, 2nd ed.; Springer: Berlin, 1993 (see pp 65−67).
(26) Fowler, P. W.; Cremona, J. E.; Steer, J. I. Systematics of bonding in nonicosahedral carbon clusters. *Theor. Chim. Acta* **1988**, *73*, 1−26.
(27) See, for example: Alexandrov, A. D. *Convex Polyheder*; Akademie-Verlag: Berlin, 1958; p 92.
(28) Wells, A. F. *Structural Inorganic Chemistry*, 4th ed.; Oxford University Press: Oxford, U.K., 1975.
(29) Shoemaker, D. P.; Shoemaker, C. B. Concerning the relative numbers of atomic coordination types in tetrahedrally close-packed metal structures. *Acta Crystallogr.* **1986**, *B42*, 3−11.
(30) Rivier, N.; Aste, T. Organised packing. In *The Kelvin problem*; Weaire, D., Ed.; Taylor & Francis: London, 1996; pp 61−68 (see especially Table 1).
(31) Sadoc, J. F.; Mosseri, R. *Frustration géométrique* (Geometric Frustration); Eyrolles: Paris, 1997 (see Chapter 7, especially Table 1).
(32) Kusner, R.; Sullivan, J. M. Comparing the Weaire-Phelan equal-volume foam to Kelvin's foam. In *The Kelvin problem*; Weaire, D., Ed.; Taylor & Francis, London, 1996, pp 71−80.
(33) Fowler, P. W. Fullerene graphs with more negative than positive eigenvalues: The exceptions that prove the rule of electron deficiency? *J. Chem. Soc., Faraday Trans.* **1997**, *93*, 1−3.
(34) Fowler, P. W.; Steer, J. I. The leapfrog principle: A rule for electron counts of carbon clusters. *J. Chem. Soc., Chem. Commun.* **1987**, 1403−1405.
(35) Manolopoulos, D. E.; Woodall, D. R.; Fowler, P. W. Electronic stability of fullerenes: Eigenvalue theorems for leapfrog carbon clusters, *J. Chem. Soc., Faraday Trans.* **1992**, *88*, 2427−2435.
(36) Fowler, P. W.; Ceulemans, A. Electron deficiency of the fullerenes. *J. Phys. Chem.* **1995**, *99*, 508−510.
(37) Yoshida, M.; Fujita, M.; Fowler, P. W.; Kirby, E. C. Nonbonding orbitals in graphite, carbon tubules, toroids and fullerenes. *J. Chem. Soc., Faraday Trans.* **1997**, *93*, 1037−1043.
(38) Fowler, P. W.; John, P. E.; Sachs, H. (3, 6) cages, hexagonal toroidal cages and their spectra. In *Discrete Mathematical Chemistry*, Hansen, P.; Fowler, P. W., Zheng, M., Eds., DIMACS Series on Discrete Mathematics and Theoretical Computer Science: AMS, 1999.
(39) For a simple geometric construction of the spectrum, see for example: Gill, G. B., Willis, M. R. *Pericyclic reactions*; Chapman and Hall: London, 1974.
(40) E. C. Kirby, Remarks upon recognising genus and possible shapes of chemical cages in the form of polyhedra, tori and Klein bottles, *Croat. Chem. Acta* **1995**, *68*, 269−282.
(41) Hilbert, D.; Cohn-Vossen, S. *Geometry and the imagination*, 2nd ed., Chelsea: New York, 1990 (see Figure 300, p 312).
(42) Cvetković, D. M.; Doob, M.; Sachs, H. *Spectra of graphs: Theory and application*; Academic Press: New York, 1979.
(43) Fowler, P. W.; Rogers, K. M. Eigenvalue spectra of leapfrog polyhedra. *J. Chem. Soc., Faraday Trans.* **1998**, *94*, 2509−2514.

CI990066H